

# UC Irvine

## UC Irvine Previously Published Works

### Title

X-ray Crystallographic Structures of Oligomers of Peptides Derived from  $\beta$ 2-Microglobulin.

### Permalink

<https://escholarship.org/uc/item/2ff5c4m5>

### Journal

Journal of the American Chemical Society, 137(19)

### Authors

Spencer, Ryan

Kreutzer, Adam

Salveson, Patrick

et al.

### Publication Date

2015-05-20

### DOI

10.1021/jacs.5b01673

Peer reviewed



# HHS Public Access

Author manuscript

*J Am Chem Soc.* Author manuscript; available in PMC 2016 May 20.

Published in final edited form as:

*J Am Chem Soc.* 2015 May 20; 137(19): 6304–6311. doi:10.1021/jacs.5b01673.

## X-ray Crystallographic Structures of Oligomers of Peptides Derived from $\beta_2$ -Microglobulin

Ryan K. Spencer, Adam G. Kreutzer, Patrick J. Salvesson, Hao Li, and James S. Nowick\*

Department of Chemistry, University of California, Irvine, Irvine

### Abstract

Amyloid diseases such as Alzheimer's disease, Parkinson's disease, and type II diabetes share common features of toxic soluble protein oligomers. There are no structures at atomic resolution of oligomers formed by full-length amyloidogenic peptides and proteins, and only a few structures of oligomers formed by peptide fragments. The paucity of structural information provides a fundamental roadblock to understanding the pathology of amyloid diseases and developing preventions or therapies. Here, we present the X-ray crystallographic structures of three families of oligomers formed by macrocyclic peptides containing a heptapeptide sequence derived from the amyloidogenic E chain of  $\beta_2$ -microglobulin ( $\beta_2m$ ). Each macrocyclic peptide contains the heptapeptide sequence  $\beta_2m63-69$  and a second heptapeptide sequence containing an *N*-methyl amino acid. These peptides form  $\beta$ -sheets that further associate into hexamers, octamers, and dodecamers: the hexamers are trimers of dimers; the octamers are tetramers of dimers; and the dodecamers contain two trimer subunits surrounded by three pairs of  $\beta$ -sheets. These structures illustrate a common theme in which dimer and trimer subunits further associate to form a hydrophobic core. The seven X-ray crystallographic structures not only illustrate a range of oligomers that a single amyloidogenic peptide sequence can form, but also how mutation can alter the size and topology of the oligomers. A cocrystallization experiment in which a dodecamer-forming peptide recruits a hexamer-forming peptide to form mixed dodecamers demonstrates that one species can dictate the oligomerization of another. These findings should also be relevant to the formation of oligomers of full-length peptides and proteins in amyloid diseases.

### Introduction

Oligomers from amyloidogenic peptides and proteins are critical in many amyloid diseases. Although the amyloidogenic peptides and proteins differ among these diseases, as do the locations within the brain and the body, the oligomers that form appear to share common features of being toxic and causing cell damage and death. Much of the understanding about amyloid oligomers has come from the  $\beta$ -amyloid peptide ( $A\beta$ ) and Alzheimer's disease.<sup>1–6</sup>

\*To whom correspondence should be addressed: jsnowick@uci.edu, Phone: (949) 824-6091. Fax: (949) 824-9920.

#### Supporting Information Available

Procedures for the synthesis and crystallization of peptides **1a–1e**, **2a–2e**, and **1aT68V**; details of X-ray diffraction data collection, processing, and refinement; details for SEC; details for MTT and LDH assays. Crystallographic data in CIF format. Crystallographic coordinates of peptides **1a**, **1b**, **1c**, **2a**, **2b**, and **1aT68V** were deposited into the Protein Data Bank (PDB) with PDB codes 4P4V, 4P4W, 4P4X, 4P4Y, 4P4Z, 4WC8, and 4X0S.

This material is available free of charge via the Internet at <http://pubs.acs.org/>.

Other amyloidogenic peptides such as  $\alpha$ -synuclein,<sup>7,8</sup> islet amyloid polypeptide (IAPP),<sup>9–11</sup> and  $\beta_2$ -microglobulin ( $\beta_2m$ )<sup>12–14</sup> are thought to form harmful oligomers in Parkinson's disease, diabetes mellitus type II, and hemodialysis-related amyloidosis. Little is known about the structures of amyloid oligomers, and there is a desperate need for atomic-resolution structures. Atomic-resolution structures of the toxic oligomers are essential to understanding the mechanisms by which they cause cell damage and death and developing effective therapies for amyloid diseases.

Many of the tools for studying the structures of amyloid oligomers have provided the molecularity and morphology of amyloid oligomers but not the structures at atomic resolution. Atomic force microscopy (AFM), transmission electron microscopy (TEM), size-exclusion chromatography (SEC), gel electrophoresis, and ion mobility mass spectrometry techniques have provided low resolution structural information about the oligomers formed by A $\beta$ . Compact spheroids have been observed by AFM and TEM.<sup>15,16</sup> Dimers, trimers, and an apparent dodecamer, isolated from the brain tissue of transgenic mice, have been observed by gel electrophoresis.<sup>4</sup> Dimers, tetramers, hexamers, and dodecamers have also been observed by ion mobility mass spectrometry.<sup>17</sup> Infrared spectroscopic studies suggest that antiparallel  $\beta$ -sheets are involved in oligomer formation.<sup>18–21</sup> While NMR and X-ray diffraction studies have provided detailed structural information about amyloid fibrils,<sup>22–27</sup> these tools are only beginning to reveal glimpses of amyloid oligomers.<sup>28–33</sup>

Full-length amyloidogenic peptides and proteins are difficult to study because they often form a heterogeneous collection of soluble oligomers and insoluble fibrils. Small hydrophobic regions of these peptides and proteins, consisting of three or more hydrophobic residues, are often responsible for the aggregation.<sup>34,35</sup> Understanding the structures formed by these smaller regions can help elucidate the structures of full-length amyloidogenic peptides and proteins. Peptide fragments containing these regions are easier to study because they can more easily form homogeneous assemblies. Eisenberg and coworkers determined the structure of an oligomer formed from the amyloidogenic region of  $\alpha B$  crystallin by X-ray crystallography.<sup>36</sup> In this structure, six  $\beta$ -strands associate to form a six-stranded hydrogen-bonded antiparallel  $\beta$ -sheet that rolls up to form a cylindrical oligomer in which hydrophobic residues comprise the inner core of the structure. Apostol, Perry, and Surewicz determined the X-ray crystallographic structure of an oligomer formed from fragments of human prion protein (PrP).<sup>37</sup> In this structure, two PrP  $\beta$ -strands are linked through a disulfide bond to form a hydrogen-bonded dimer. Six dimers associate along the hydrogen-bonding edges to form a cylindrical hexamer with hydrophobic residues comprising the inner core of the structure. Our laboratory has determined the X-ray crystallographic structure of an oligomer formed by a macrocyclic peptide derived from A $\beta$ . In this structure, the peptide folds into an antiparallel  $\beta$ -sheet and assembles to form triangular trimers and higher-order oligomers.<sup>38</sup>

In the current study, we set out to use X-ray crystallography to explore the range of oligomers that a single amyloidogenic peptide sequence can form.<sup>39</sup> We designed macrocyclic peptides **1** and **2** to incorporate the amyloidogenic heptapeptide sequence YLLYYTE ( $\beta_2m_{63–69}$ ) from the aggregation-prone E chain of  $\beta_2m$  and fold into an antiparallel  $\beta$ -sheet (Figure 1).<sup>40–42</sup> The peptide contains a second heptapeptide sequence with an *N*-methyl

amino acid, as a template strand to block uncontrolled aggregation.<sup>43</sup> The two heptapeptides are connected by two  $\delta$ -linked ornithine turn units, which act as  $\beta$ -turn mimics and reinforce  $\beta$ -sheet formation.<sup>44</sup> We replaced Tyr<sub>66</sub> of  $\beta_2m_{63-69}$  with a *p*-iodophenylalanine to determine the X-ray crystallographic phases. We used Lys residues at the R<sub>1</sub> and R<sub>7</sub> positions of the template  $\beta$ -strand to enhance solubility, Val residues at the R<sub>2</sub> and R<sub>6</sub> positions to enhance  $\beta$ -sheet formation, and an *N*-methyl amino acid at the R<sub>4</sub> position to prevent fibril formation and promote oligomer formation.

We kept the  $\beta_2m_{63-69}$  peptide strand constant and varied residues R<sub>3</sub>, R<sub>4</sub>, and R<sub>5</sub> to explore the effects of residue size and hydrophobicity on oligomer formation. Peptides **1** and **2** present two surfaces: a major surface that displays the side chains of eight amino acids and a minor surface that displays the side chains of six amino acids (shown by the blue side chains and red side chains in Figure 1). The major surface displays Tyr<sub>63</sub>, Leu<sub>65</sub>, Tyr<sub>67</sub>, and Glu<sub>69</sub> of  $\beta_2m_{63-69}$ , while the minor surface displays Leu<sub>64</sub>, Phe<sub>66</sub><sup>I</sup> and Thr<sub>68</sub>. The major surface also displays Lys<sub>1</sub>, R<sub>3</sub>, R<sub>5</sub>, and Lys<sub>7</sub> of the template strand, while the minor surface displays Val<sub>2</sub>, R<sub>4</sub>, and Val<sub>6</sub>. We initially synthesized and studied ten peptides. In five we incorporated alanine at positions R<sub>3</sub> and R<sub>5</sub> (**1a–1e**); in five we incorporated threonine at positions R<sub>3</sub> and R<sub>5</sub> (**2a–2e**). In each series, we varied the *N*-methylated residue R<sub>4</sub>, to incorporate *N*-methylated alanine, valine, leucine, isoleucine, and norleucine (Nle). Table 1 summarizes the peptides we synthesized and the oligomers we observed by X-ray crystallography.

## Results

Five of the ten peptides afforded crystals suitable for X-ray crystallography. Their X-ray crystallographic structures reveal three families of oligomers: hexamers, octamers, and dodecamers (Figures 3, 4, and 5). Peptides **1a** and **2a** form hexamers, peptide **2b** forms an octamer, and peptides **1b** and **1c** form dodecamers. These oligomers are composed of monomer subunits with common structures that assemble in different ways. In each of the monomer subunits, the  $\beta_2m_{63-69}$  and template strands hydrogen bond together to form a  $\beta$ -sheet. The  $\beta$ -sheets have a strong right-handed twist of about 13–22 degrees per residue along the  $\beta$ -strand axis, and thus mimic twisted  $\beta$ -hairpins.

The  $\beta$ -hairpins are fully hydrogen bonded, except between Glu<sub>69</sub> and Lys<sub>1</sub>, in which the hydroxyl group of Thr<sub>68</sub> can disrupt the hydrogen bonding between these two residues (Figure 2A–D). To probe the effect of the hydroxyl group on  $\beta$ -hairpin structure and oligomer formation, we prepared a homologue of peptide **1a** with Val in place of Thr<sub>68</sub> (peptide **1a<sub>T68V</sub>**). The X-ray crystallographic structure of this homologue shows a fully hydrogen-bonded  $\beta$ -hairpin (Figure 2E and F) and no appreciable difference in the structure of the oligomers that form, which are hexamers in both cases (Figure S1).

## Hexamer

Peptide **1a** crystallizes from 0.1 M Tris buffer at pH 8.0 with 0.3 M Li<sub>2</sub>SO<sub>4</sub> and 45% PEG 400, in the *P4<sub>2</sub>22* space group, with three nearly identical  $\beta$ -hairpin monomers in the asymmetric unit (ASU). Expanding the ASU to generate the lattice shows hexamers composed of six  $\beta$ -hairpins assembled as a trimer of dimers (Figure 3). In each dimer, two  $\beta$ -

hairpins come together through edge-to-edge interactions between the  $\beta_{2m}$  strands to form a four-stranded antiparallel  $\beta$ -sheet (Figure 3B). Residues Leu<sub>64</sub>, Phe<sup>I</sup><sub>66</sub>, and Thr<sub>68</sub> of one monomer form hydrogen-bonded pairs with residues Thr<sub>68</sub>, Phe<sup>I</sup><sub>66</sub>, and Leu<sub>64</sub> of the other monomer. Hydrophobic contacts between the side chains of residues Tyr<sub>63</sub>, Leu<sub>65</sub>, and Glu<sub>69</sub>, appear to further stabilize the dimer.

Three antiparallel  $\beta$ -sheet dimers come together through face-to-face interactions around a central 3-fold axis to form the hexamer (Figure 3C and 3D). The minor surfaces of the  $\beta$ -hairpins face inward to form the hydrophobic core of the hexamer, while the major surfaces face outward and are exposed to solvent within the lattice. The six hydrophobic Phe<sup>I</sup><sub>66</sub> residues comprise the center of the hydrophobic core, stacking in pairs, and forming additional hydrophobic contacts among the edges of the aromatic rings. Residues Leu<sub>64</sub>, Val<sub>2</sub>, *N*-Me Ala<sub>4</sub>, and Val<sub>6</sub> of the minor faces surround the iodophenyl groups and complete the hydrophobic core (Figure 3E and 3F).

Peptides **2a** and **1a<sub>T68V</sub>** also crystallize as hexamers from conditions similar to peptide **1a**, but in the *R32* space group. The ASU of peptide **2a** contains seven  $\beta$ -hairpin monomers; the ASU of peptide **1a<sub>T68V</sub>** contains only one. The hexamers formed by peptides **2a** and **1a<sub>T68V</sub>** are nearly identical to those formed by peptide **1a**.

### Octamer

Peptide **2b** crystallizes from 0.1 M SPG (succinic acid-phosphate-glycine) buffer at pH 10.0 and 35% PEG 1500, in the *P4<sub>3</sub>2<sub>1</sub>2* space group, with 12  $\beta$ -hairpin monomers in the ASU. Expanding the ASU to generate the lattice shows octamers composed of eight  $\beta$ -hairpins assembled as a tetramer of dimers (Figure 4). In each dimer, two  $\beta$ -hairpins associate along the residues of the  $\beta_{2m}$  strand and interact through face-to-face contacts to form a facial dimer (Figure 4B). The two  $\beta$ -hairpins are oriented in an antiparallel fashion, like those in the hexamer, but interact through hydrophobic contacts among the side chains of Leu<sub>64</sub>, Phe<sup>I</sup><sub>66</sub>, Val<sub>2</sub>, and *N*-Me Val<sub>4</sub>, rather than through hydrogen bonding between the main chains of the  $\beta$ -hairpins.

Four facial dimers associate around a 4-fold axis to form the octamer. The minor surfaces of the  $\beta$ -hairpins face inward to form the hydrophobic core of the octamer, while the major surfaces face outward and are exposed to solvent within the lattice (Figure 4C and 4D). The Phe<sup>I</sup><sub>66</sub> pairs of the facial dimers comprise the center of the octamer. Residues Leu<sub>64</sub>, Val<sub>2</sub>, *N*-Me Val<sub>4</sub>, and Val<sub>6</sub> of the minor surfaces make up the rest of the hydrophobic core, with Val<sub>2</sub> and *N*-Me Val<sub>4</sub> surrounding the iodophenyl groups and residues Leu<sub>64</sub> and Val<sub>6</sub> packing in layers above and below the iodophenyl groups (Figure 4E and 4F). Salt-bridges between Lys<sub>1</sub> and Glu<sub>69</sub> residues and a network of hydrogen bonds between the edges of the  $\beta$ -hairpins of the four dimer subunits further stabilize the octamer.

### Dodecamer

Peptide **1b** crystallizes from 0.1 M Tris buffer at pH 8.0 and 1.5 M (NH<sub>4</sub>)<sub>2</sub>SO<sub>4</sub>, in the *P3<sub>1</sub>21* space group, with 12  $\beta$ -hairpins in the ASU. Expanding the ASU to generate the crystal lattice shows dodecamers composed of twelve  $\beta$ -hairpins. The dodecamer contains a dimer

of trimers, which makes a central hexamer, and three additional pairs of  $\beta$ -hairpins, which surround the central hexamer (Figure 5).

In the trimer, three  $\beta$ -hairpins associate in a triangular fashion through the edges of the  $\beta_2m$  strands (Figure 5B). The  $\beta_2m$  strands hydrogen bond together at the corners of the triangles, with Leu<sub>64</sub> and the proximal ornithine hydrogen bonding with Phe<sup>I</sup><sub>66</sub> and Thr<sub>68</sub> at each corner. Three ordered waters fill the hole in the center of the triangle and form additional hydrogen bonds with Leu<sub>64</sub> and Phe<sup>I</sup><sub>66</sub> thus creating a network that satisfies all of the hydrogen-bonding valences of the  $\beta_2m$  strands. Hydrophobic contacts among the side-chains of the  $\beta$ -hairpins further stabilize the trimer structure.

Two triangular trimers come together through face-to-face interactions to form the central hexamer within the dodecamer. The minor surfaces of the  $\beta$ -hairpins face inward and contribute to the hydrophobic core of the dodecamer, while the major surfaces face outward and are exposed to solvent within the lattice. The Phe<sup>I</sup><sub>66</sub> residues of the opposing trimers stack in the center of the hydrophobic core, and the hydrophobic side chains of Leu<sub>64</sub>, Val<sub>2</sub>, *N*-Me Val<sub>4</sub>, and Val<sub>6</sub> surround the iodophenyl groups. The minor surfaces of the three pairs of  $\beta$ -hairpins that surround the central hexamer face inward and extend the hydrophobic core through additional hydrophobic contacts. These pairs of  $\beta$ -hairpins do not hydrogen bond to each other, but are stabilized by hydrophobic contacts with the hexamer through the residues of the minor surfaces (Figure 5E and 5F).

Peptide **1c** also crystallizes as dodecamers, but from 0.1 M Tris at pH 7.5 with 0.2 M Li<sub>2</sub>SO<sub>4</sub> and 25% PEG 400, in the *P*4<sub>1</sub>22 space group, with 12  $\beta$ -hairpins forming a dodecamer in the ASU. The dodecamers formed by peptide **1c** are nearly identical to those formed by peptide **1b**.

### A Mixed Dodecamer

We cocrystallized peptides **1a** and **1c** to ask what would happen when peptides that formed two different oligomers (hexamers and dodecamers) were allowed to crystallize from a 1:1 mixture. Much to our surprise, the two peptides cocrystallized as a dodecamer similar to that of peptide **1c**, but with peptide **1c** forming the central hexamer and peptide **1a** forming the three pairs of  $\beta$ -hairpins surrounding the hexamer (Figure 6). Peptides **1a** and **1c** cocrystallize under conditions similar to those from which **1a** and **1c** crystallize individually: 0.1 M Tris buffer at pH 7.5 with 0.2 M Li<sub>2</sub>SO<sub>4</sub> and 30% PEG 400, in the *P*4<sub>1</sub>22 space group, with 12  $\beta$ -hairpins forming a dodecamer in the asymmetric unit (ASU). The formation of a mixed dodecamer from peptides with propensities to form different oligomers demonstrates that the oligomers formed by one peptide may alter the oligomerization of another peptide.

### Size-Exclusion Chromatography of Peptides 1 and 2

Size-exclusion chromatography (SEC) studies indicate that peptides **1** and **2** form oligomers in solution. SEC was performed on 1 mM solutions of peptides **1** and **2** in 0.1 M phosphate buffer at pH 7.4 with a Superdex 200 column. The elution profiles were compared to those of size standards vitamin B12, ribonuclease A, and chymotrypsinogen. These 1.3, 13.7, and

25.6 kDa size standards eluted at 20.3, 17.3, and 16.5 mL, respectively. Peptides **1b–1e** and **2a–2e** elute between 17.3 to 18.0 mL (Table 2; Figures S3B–S12B). (Peptide 1a precipitates from phosphate buffer; SEC of the supernatant gives a weak signal and slightly larger elution volume.) These volumes are substantially lower than would be expected for the corresponding 2.0 kDa monomers. The elution volumes of peptides **1b–1e** and **2a–2e** are similar to that of ribonuclease A. These volumes are consistent with oligomers in the hexamer to octamer size range, for both the peptides that crystallize and those that do not. The peak shapes of the peptides are slightly broader than those of the size standards and the peaks tail slightly, reflecting an oligomer-monomer equilibrium in which the oligomer predominates. Peptides 1b and 1c do not appear to elute as dodecamers, suggesting that the central hexamer elutes without the three peripheral pairs of  $\beta$ -hairpins observed in the crystal lattice. Figure 7 shows representative SEC chromatograms of peptides **2a**, **2b**, and **1b**, which form hexamers, octamers, and dodecamers in the crystal lattice.

### Cytotoxicity of Peptides 1 and 2

We studied the cytotoxicity of peptides **1** and **2** using MTT conversion and lactate dehydrogenase (LDH) release assays in the neuroblastoma cell line SH-SY5Y. At 25  $\mu$ M, peptides **1** and **2** showed a range of toxicities, with peptides **1a**, **1c**, **1e**, **2c**, and **2e** being more toxic and peptides **1b**, **1d**, **2a**, **2b**, and **2d** being less toxic (Table 2; Figure S2). These differences do not correlate with the crystallographic observation of oligomers. Two of the peptides that crystallize are more toxic (1a and 1c), while three that crystallize are less toxic (**1b**, **2a**, and **2b**). Three of the peptides that do not crystallize are more toxic (**1e**, **2c**, and **2e**), while two that do not crystallize are less toxic (**1d** and **2d**). The differences in toxicity do not correlate with oligomer structure. One peptide that crystallizes as a hexamer (1a) is more toxic, while the other peptide that crystallizes as a hexamer (**2a**) is less toxic. One peptide that crystallizes as a dodecamer (**1c**) is more toxic, while the other peptide that crystallizes as a dodecamer (**1b**) is less toxic. The peptide that crystallizes as an octamer (**2b**) is less toxic. The differences also do not correlate with the hydrophobicity of the peptides. In the series with Ala at positions R<sub>3</sub> and R<sub>5</sub>, the less hydrophobic peptide **1a** (R<sub>4</sub> = Ala) and more hydrophobic peptides 1c and 1e (R<sub>4</sub> = Leu and Nle) are more toxic. Peptide **1d** (R<sub>4</sub> = Ile) is comparable in hydrophobicity to **1c** and **1e** but is less toxic. Similar differences are observed in the series with Thr at positions R<sub>3</sub> and R<sub>5</sub>, with **2c** and **2e** (R<sub>4</sub> = Leu and Nle) being more toxic, and **2a**, **2b**, and **2d** (R<sub>4</sub> = Ala, Val, and Ile) being less toxic. The differences in the observed toxicities might reflect differences in propensities of the peptides to form oligomers at concentrations 1-2 orders of magnitude lower than those used for crystallization and SEC studies.

### Discussion

The seven X-ray crystallographic structures presented here illustrate a range of oligomers that a single amyloidogenic peptide sequence can form. Although the hexamers, octamers, and dodecamers differ in size and topology, they share a common theme of a globular structure with a hydrophobic core. The hydrophobic core is formed by hydrophobic side chains of  $\beta$ -hairpins, which form dimer and trimer subunits within the oligomers. The hexamers and octamers formed by peptides **1a**, **1a<sub>T68V</sub>**, **2a**, and **2b** comprise three or four

dimers packed around a central hydrophobic core and thus resemble the hexamer derived from PrP.<sup>37</sup> The dodecamers formed by peptides **1b** and **1c** and by a mixture of **1a** and **1c** differ substantially from the hexamers and octamers, because they are based on a pair of triangular trimers surrounded by three pairs of  $\beta$ -hairpins. We have previously observed similar triangular trimers in the X-ray crystallographic structures of peptides derived from A $\beta$ <sub>17-36</sub>.<sup>38</sup> Based on these observations, we now believe that the formation of higher-order oligomers from these types of dimer and trimer building blocks is a common feature of many amyloidogenic peptides and proteins. Central to the formation of all of these compact globular oligomers are twisted  $\beta$ -hairpins, which differ from the relatively flat  $\beta$ -sheets that make up fibrils.

Small differences in peptide sequence can lead to large differences in oligomer structure. The  $\beta$ -hairpins formed by peptides **1** and **2** are nearly identical to each other, yet they arrange in various alignments to form three families of oligomers — hexamers, octamers, and dodecamers. There is little obvious relationship between the hydrophobicity and size of residues R<sub>3</sub>–R<sub>5</sub> and the oligomers that form. Peptides with both hydrophobic (Ala) and hydrophilic (Thr) residues at R<sub>3</sub> and R<sub>5</sub> (**1a** and **2a**) permit hexamer formation. Either dodecamer or octamer (**1b** or **2b**) form when R<sub>4</sub> is increased in size (Ala to Val). Further increasing the size of R<sub>4</sub> (Val to Leu; **1b** to **1c**) does not alter dodecamer formation. Other changes in R<sub>3</sub> and R<sub>5</sub> (**1c** to **2c**) or R<sub>4</sub> (Ile, Nle; **1d**, **1e**, **2d**, **2e**) give peptides that do not crystallize. Although we do not yet understand the relationship between the residue hydrophobicities and sizes and the oligomer structures, it is clear that the R<sub>4</sub> residue is important for oligomer formation. Increasing the size of the side chain at the R<sub>4</sub> position may change the packing of the hydrophobic core and thus change which oligomer forms.

The changes from hexamer to octamer to dodecamer that occur upon mutating a single residue may provide insights into the effects of familial mutations in amyloid diseases. Changing an alanine in peptide **1a** to valine or leucine in peptides **1b** and **1c** changes a hexamer to a dodecamer; changing an alanine in peptide **2a** to valine in peptide **2b** changes a hexamer to an octamer. These changes are similar to the point mutations that dictate early onset in Alzheimer's disease and in the synucleinopathies related to Parkinson's disease.<sup>45,46</sup> It is quite possible that the mutant A $\beta$  peptides and  $\alpha$ -synuclein protein associated with these heritable diseases also form different oligomers than those formed by the non-mutant wild types, and that these differences in oligomer structure may alter the toxicity of the oligomers. The formation of the a mixed dodecamer from peptides **1a** and **1c** is especially intriguing, because it demonstrates that a mutant peptide or protein can dictate the structure of the oligomers that form. Similar effects may occur in individuals with a single allele for a familial mutation, and the resulting mutant peptide or protein may recruit the wild-type peptide or protein to form mixed oligomers with different oligomerization states and more toxic structures.

## Conclusion

Macrocyclic peptides that mimic  $\beta$ -hairpins and contain an amyloidogenic peptide sequence and an *N*-methyl amino acid are valuable for exploring the structure and assembly of amyloid oligomers. These peptides are easy to synthesize and are often easy to crystallize.



X-ray crystallography readily reveals the structures of the oligomers to consist of dimer and trimer subunits that assemble to create a hydrophobic core. These common structural features should also occur in the oligomers formed by full-length amyloidogenic peptides and proteins. Although the studies described here use an amyloidogenic peptide sequence from  $\beta_2m$ , the modes of oligomer assembly observed likely transcend individual peptide sequences and represent some of the structural diversity among amyloid oligomers.

The three families of oligomers observed — hexamers, octamers, and dodecamers — illustrate some of the polymorphism of amyloid oligomers and highlight the impact that a single mutation can have on oligomer structure. The formation of the mixed dodecamer illustrates the potential of one amyloidogenic peptide or protein to dictate oligomer formation by another. This observation may have important implications for the role of heritable mutations in familial amyloid diseases and may also be relevant to interactions among different amyloidogenic peptides and proteins, such as A $\beta$ , tau,  $\alpha$ -synuclein, and IAPP, in amyloid diseases.

## Supplementary Material

Refer to Web version on PubMed Central for supplementary material.

## Acknowledgments

We thank Professors Thomas L. Poulos and Kim N. Green and Drs. Huiying Li and Nicholas Chim for helpful discussions and thoughtful comments. This work was supported by the National Institutes of Health (Grant 5R01GM097562) and the National Science Foundation (CHE-1058825). Use of the Berkeley Center for Structural Biology (BCSB) beamlines of the Advanced Light Source (ALS) is supported by the National Institutes of Health (NIGMS), the Howard Hughes Medical Institute, and the Department of Energy. Use of the Stanford Synchrotron Radiation Lightsource (SSRL) is supported by the Department of Energy and the National Institutes of Health (NIGMS).

## References

1. Walsh DM, Klyubin I, Fadeeva JV, Cullen WK, Anwyl R, Wolfe MS, Rowan MJ, Selkoe DJ. *Nature*. 2002; 416:535–539. [PubMed: 11932745]
2. Cleary JP, Walsh DM, Hofmeister JJ, Shankar GM, Kuskowski MA, Selkoe DJ, Ashe KH. *Nat Neurosci*. 2005; 8:79–84. [PubMed: 15608634]
3. Townsend M, Shankar GM, Mehta T, Walsh DM, Selkoe DJ. *J Physiol*. 2006; 572:477–492. [PubMed: 16469784]
4. Lesné S, Koh MT, Kotilinek L, Kaye R, Glabe CG, Yang A, Gallagher M, Ashe KH. *Nature*. 2006; 440:352–357. [PubMed: 16541076]
5. Zhao W-Q, De Felice FG, Fernandez S, Chen H, Lambert MP, Quon MJ, Krafft GA, Klein WL. *FASEB J*. 2008; 22:246–260. [PubMed: 17720802]
6. Haass C, Selkoe DJ. *Nat Rev Mol Cell Biol*. 2007; 8:101–112. [PubMed: 17245412]
7. Caughey B, Lansbury PT. *Annu Rev Neurosci*. 2003; 26:267–298. [PubMed: 12704221]
8. Winner B, Jappelli R, Maji SK, Desplats PA, Boyer L, Aigner S, Hetzer C, Loher T, Vilar M, Campion S, Tzitzilonis C, Soragni A, Jessberger S, Mira H, Consiglio A, Pham E, Masliah E, Gage FH, Riek R. *Proc Natl Acad Sci USA*. 2011; 108:4194–4199. [PubMed: 21325059]
9. Lin CY, Gurlo T, Kaye R, Butler AE, Haataja L, Glabe CG, Butler PC. *Diabetes*. 2007; 56:1324–1332. [PubMed: 17353506]
10. Haataja L, Gurlo T, Huang CJ, Butler PC. *Endocr Rev*. 2008; 29:303–316. [PubMed: 18314421]

11. Gurlo T, Ryazantsev S, Huang CJ, Yeh MW, Reber HA, Hines OJ, O'Brien TD, Glabe CG, Butler PC. *Am J Pathol.* 2010; 176:861–869. [PubMed: 20042670]
12. Eakin CM, Attenello FJ, Morgan CJ, Miranker AD. *Biochemistry.* 2004; 43:7808–7815. [PubMed: 15196023]
13. Mustata M, Capone R, Jang H, Arce FT, Ramachandran S, Lal R, Nussi-nov R. *J Am Chem Soc.* 2009; 131:14938–14945. [PubMed: 19824733]
14. Smith DP, Radford SE, Ashcroft AE. *Proc Natl Acad Sci USA.* 2010; 107:6794–6798. [PubMed: 20351246]
15. Chromy BA, Nowak RJ, Lambert MP, Viola KL, Chang L, Velasco PT, Jones BW, Fernandez SJ, Lacor PN, Horowitz P, Finch CE, Krafft GA, Klein WL. *Biochemistry.* 2003; 42:12749–12760. [PubMed: 14596589]
16. Ahmed M, Davis J, Aucoin D, Sato T, Ahuja S, Aimoto S, Elliott JI, Van Nostrand WE, Smith SO. *Nat Struct Mol Biol.* 2010; 17:561–567. [PubMed: 20383142]
17. Bernstein SL, Dupuis NF, Lazo ND, Wyttenbach T, Condron MM, Bitan G, Teplow DB, Shea JE, Ruotolo BT, Robinson CV, Bowers MT. *Nat Chem.* 2009; 1:326–331. [PubMed: 20703363]
18. Cerf E, Sarroukh R, Tamamizu-Kato S, Breydo L, Derclaye S, Dufrene YF, Narayanaswami V, Goormaghtigh E, Ruyschaert JM, Raussens V. *Biochem J.* 2009; 421:415–423. [PubMed: 19435461]
19. Bleiholder C, Dupuis NF, Wyttenbach T, Bowers MT. *Nat Chem.* 2011; 3:172–177. [PubMed: 21258392]
20. Celej MS, Sarroukh R, Goormaghtigh E, Fidelio GD, Ruyschaert JM, Raussens V. *Biochem J.* 2012; 443:719–726. [PubMed: 22316405]
21. Buchanan LE, Dunkelberger EB, Tran HQ, Cheng PN, Chiu CC, Cao P, Raleigh DP, de Pablo JJ, Nowick JS, Zanni MT. *Proc Natl Acad Sci USA.* 2013; 110:19285–19290. [PubMed: 24218609]
22. Petkova AT, Yau W-M, Tycko R. *Biochemistry.* 2006; 45:498–512. [PubMed: 16401079]
23. Paravastu AK, Leapman RD, Yau WM, Tycko R. *Proc Natl Acad Sci USA.* 2008; 105:18349–18354. [PubMed: 19015532]
24. Lu J-X, Qiang W, Yau W-M, Schwieters CD, Meredith SC, Tycko R. *Cell.* 2013; 154:1257–1268. [PubMed: 24034249]
25. Lührs T, Ritter C, Adrian M, Riek-Loher D, Bohrmann B, Dbeli H, Schu-bert D, Riek R. *Proc Natl Acad Sci USA.* 2005; 102:17342–17347. [PubMed: 16293696]
26. Iwata K, Fujiwara T, Matsuki Y, Akutsu H, Takahashi S, Naiki H, Goto Y. *Proc Natl Acad Sci USA.* 2006; 103:18119–18124. [PubMed: 17108084]
27. Jahn TR, Makin OS, Morris KL, Marshall KE, Tian P, Sikorski P, Serpell LC. *J Mol Biol.* 2010; 395:717–727. [PubMed: 19781557]
28. Chimon S, Shaibat MA, Jones CR, Calero DC, Aizezi B, Ishii Y. *Nat Struct Mol Biol.* 2007; 14:1157–1164. [PubMed: 18059284]
29. Scheidt HA, Morgado I, Rothmund S, Huster D, Fändrich M. *Angew Chem Int Ed Engl.* 2011; 50:2837–2840. [PubMed: 21387500]
30. Tay WM, Huang D, Rosenberry TL, Paravastu AK. *J Mol Biol.* 2013; 425:2494–2508. [PubMed: 23583777]
31. Sarkar B, Mithu VS, Chandra B, Mandal A, Chandrakesan M, Bhowmik D, Madhu PK, Maiti S. *Angew Chem Int Ed Engl.* 2014; 53:6888–6892. [PubMed: 24756858]
32. Lendel C, Bjerring M, Dubnovitsky A, Kelly RT, Filippov A, Antzutkin ON, Nielsen NC, Härd T. *Angew Chem Int Ed Engl.* 2014; 53:12756–12760. [PubMed: 25256598]
33. Huang D, Zimmerman MI, Martin PK, Nix AJ, Rosenberry TL, Paravastu AK. *J Mol Biol.* 201510.1016/j.jmb.2015.04.004
34. Pawar AP, Dubay KF, Zurdo J, Chiti F, Vendruscolo M, Dobson CM. *J Mol Biol.* 2005; 350:379–392. [PubMed: 15925383]
35. Tzotzos S, Doig AJ. *Protein Science.* 2010; 19:327–348. [PubMed: 20027621]
36. Laganowsky A, Liu C, Sawaya MR, Whitelegge JP, Park J, Zhao M, Pen-salfini A, Soriaga AB, Landau M, Teng PK, Cascio D, Glabe C, Eisenberg D. *Science.* 2012; 335:1228–1231. [PubMed: 22403391]

37. Apostol MI, Perry K, Surewicz WK. *J Am Chem Soc.* 2013; 135:10202–10205. [PubMed: 23808589]
38. Spencer RK, Li H, Nowick JS. *J Am Chem Soc.* 2014; 136:5595–5598. [PubMed: 24669800]
39. Spencer RK, Nowick JS. *Isr J Chem.* 2015;10.1002/ijch.201400179
40. Trinh CH, Smith DP, Kalverda AP, Phillips SE, Radford SE. *Proc Natl Acad Sci USA.* 2002; 99:9771–9776. [PubMed: 12119416]
41. Jones S, Manning J, Kad NM, Radford SE. *J Mol Biol.* 2003; 325:249–257. [PubMed: 12488093]
42. Ivanova MI, Thompson MJ, Eisenberg D. *Proc Natl Acad Sci USA.* 2006; 103:4079–4082. [PubMed: 16537488]
43. Spencer R, Chen KH, Manuel G, Nowick JS. *Eur J Org Chem.* 2013; 2013:3523–3528.
44. Nowick JS, Brower JO. *J Am Chem Soc.* 2003; 125:876–877. [PubMed: 12537479]
45. Karran E, Mercken M, De Strooper B. *Nat Rev Drug Discov.* 2011; 10:698–712. [PubMed: 21852788]
46. Bendor JT, Logan TP, Edwards RH. *Neuron.* 2013; 79:1044–1066. [PubMed: 24050397]

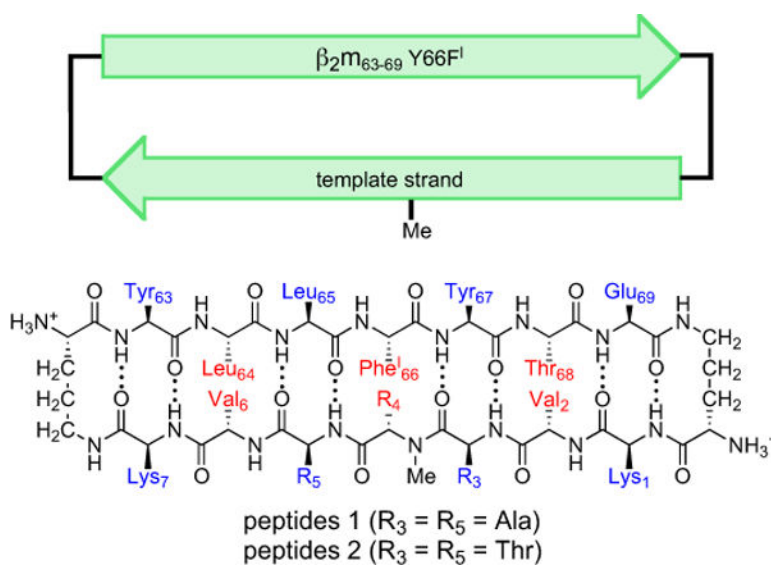


**Figure 1.**  
Cartoon and chemical structures of peptides **1** and **2**.

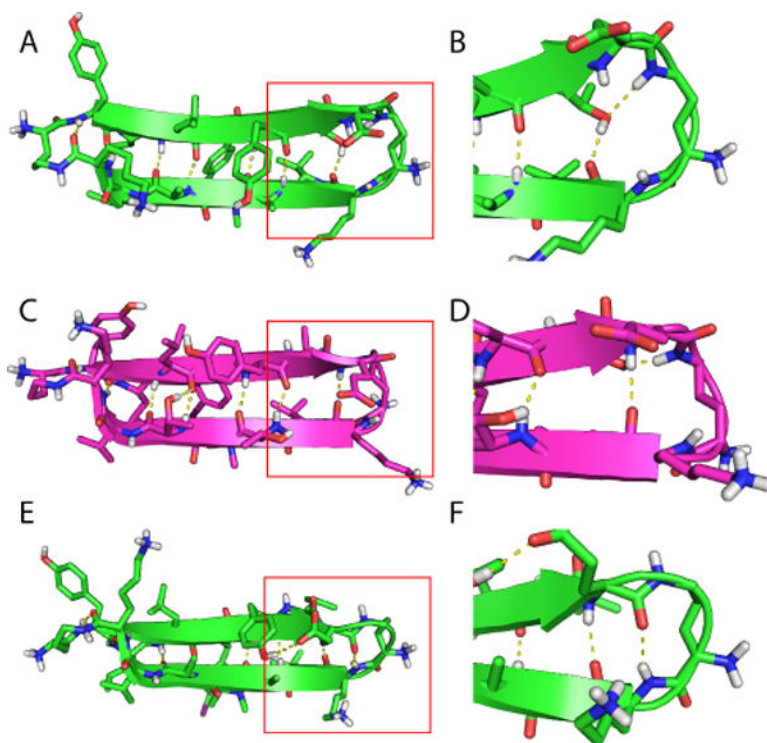


**Figure 2.**

X-ray crystallographic structure of  $\beta$ -hairpins formed by peptides **1a** **2b** and **1a<sub>T68V</sub>**. (A)  $\beta$ -Hairpin formed by peptide **1a**. (B) Detail showing the hydroxyl group of Thr<sub>68</sub> hydrogen bonding with the carbonyl of the adjacent Lys<sub>1</sub> residue. (C)  $\beta$ -Hairpin formed by peptide **2b**. (D) Detail showing the hydroxyl group of Thr<sub>68</sub> hydrogen bonding with the NH of ornithine. (E)  $\beta$ -Hairpin formed by peptide **1a<sub>T68V</sub>**. (F) Detail showing the hydrogen bonding between residues Glu<sub>68</sub> and Lys<sub>1</sub>.

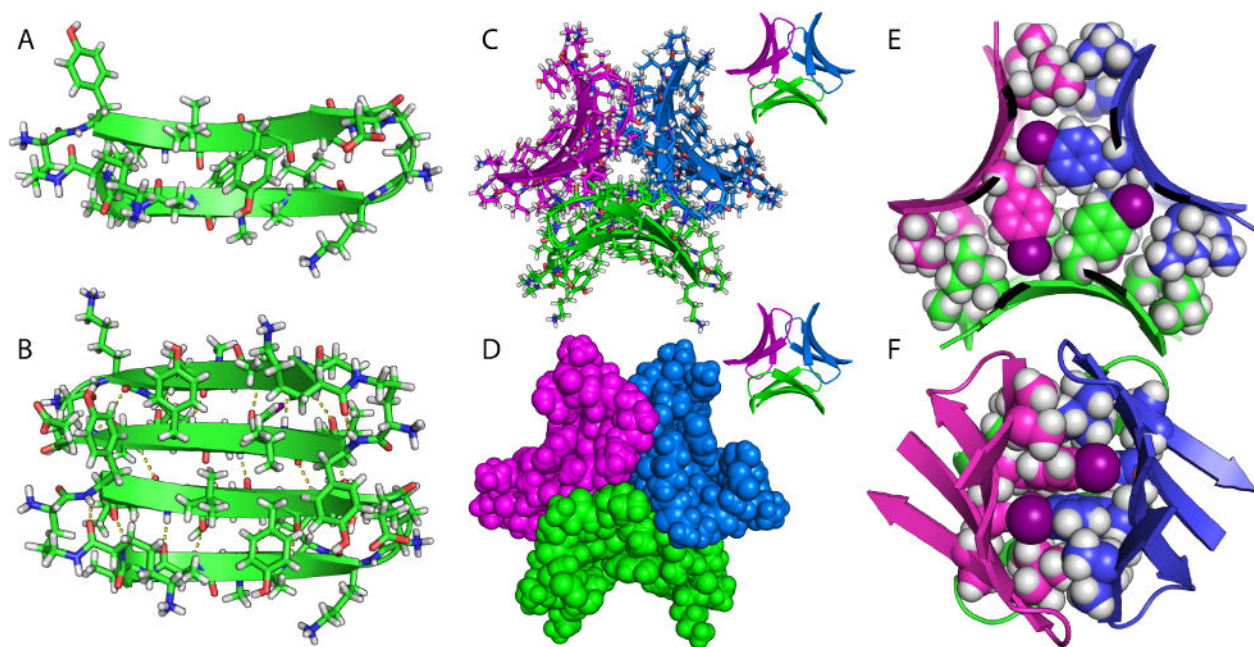


**Figure 3.** X-ray crystallographic structure of peptide **1a** (hexamer). (A)  $\beta$ -Hairpin monomer. (B) Antiparallel  $\beta$ -sheet dimer. (C) Hexamer top view (cartoon and sticks). (D) Hexamer top view (spheres). (E) Hydrophobic core top view (Val<sub>2</sub> and *N*-Me Ala<sub>4</sub> omitted). (F) Hydrophobic core side view (Val<sub>6</sub> omitted).

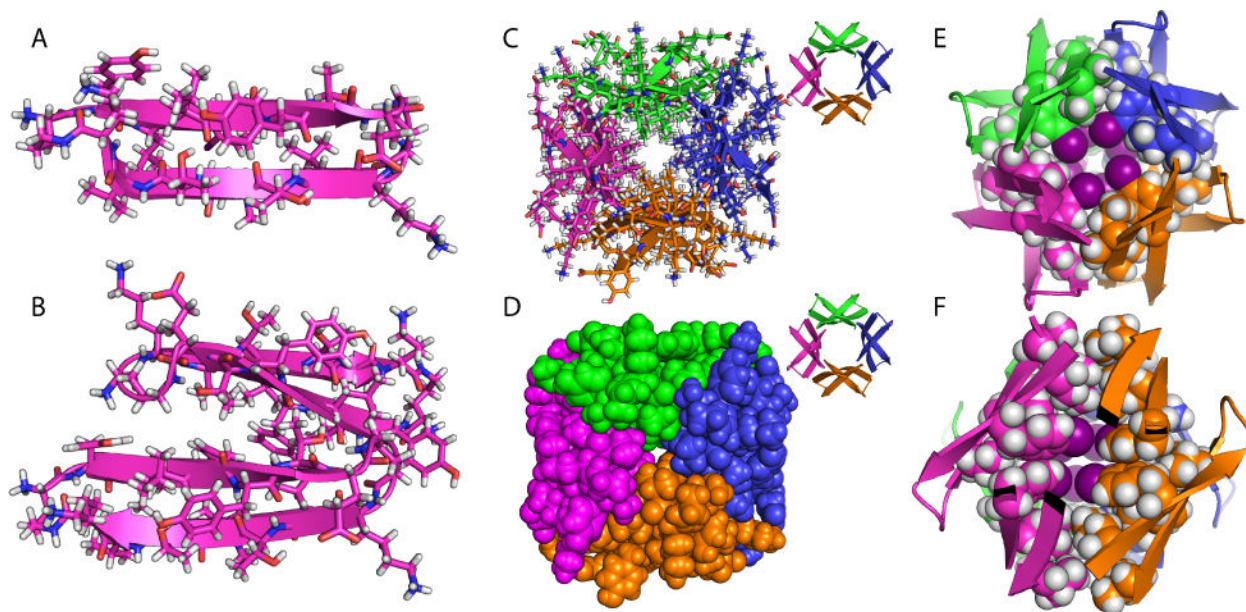


**Figure 4.** X-ray crystallographic structure of peptide **2b** (octamer). (A)  $\beta$ -Hairpin monomer. (B) Facial dimer. (C) Octamer top view (cartoon and sticks). (D) Octamer top view (spheres). (E) Hydrophobic core top view (Leu<sub>64</sub> and Val<sub>6</sub> omitted). (F) Hydrophobic core side view (Val<sub>2</sub> omitted).

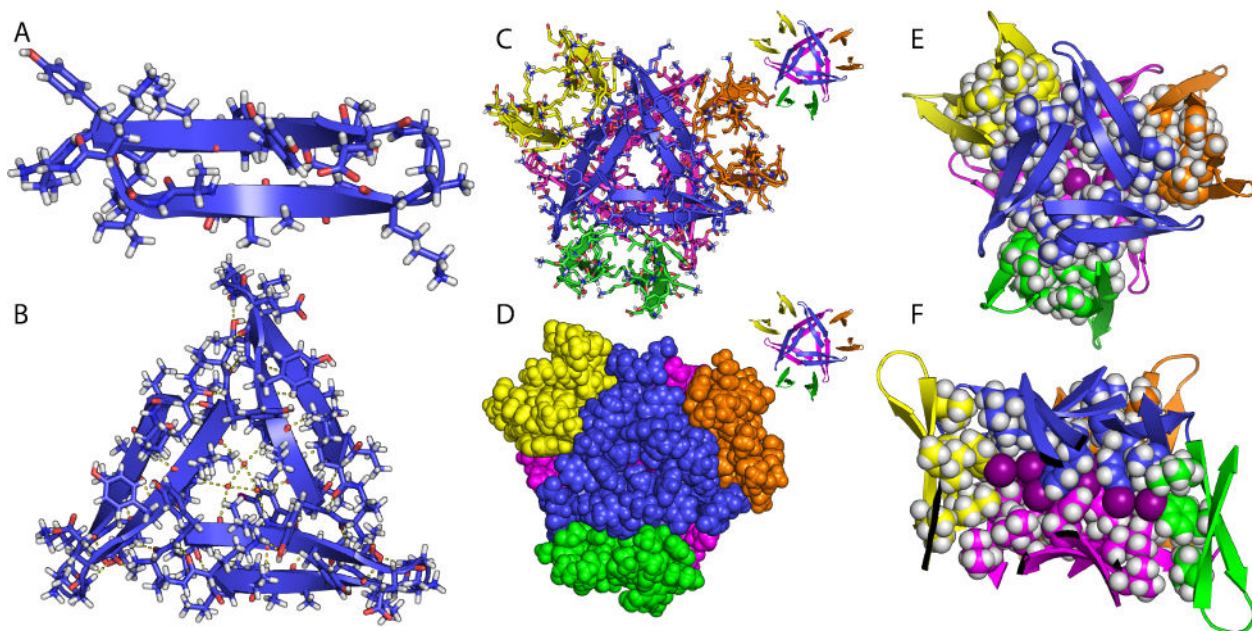


**Figure 5.** X-ray crystallographic structure of peptide **1b** (dodecamer). (A)  $\beta$ -Hairpin monomer. (B) Triangular trimer. (C) Dodecamer top view (cartoon and sticks). (D) Dodecamer top view (spheres). (E) Hydrophobic core top view. (F) Hydrophobic core side view (cutaway).



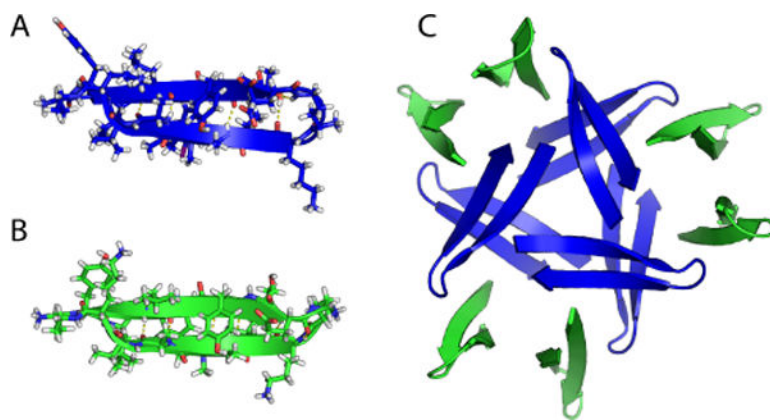


**Figure 6.** X-ray crystallographic structure of a mixed dodecamer formed by peptides **1a** and **1c**. (A)  $\beta$ -Hairpin formed by peptide **1c**. (B)  $\beta$ -Hairpin formed by peptide **1a**. (C) Mixed dodecamer with six  $\beta$ -hairpins of peptide **1c** (blue) forming the central hexamer (dimer of trimers) and three pairs of  $\beta$ -hairpins of peptide **1a** (green) surrounding the central hexamer.

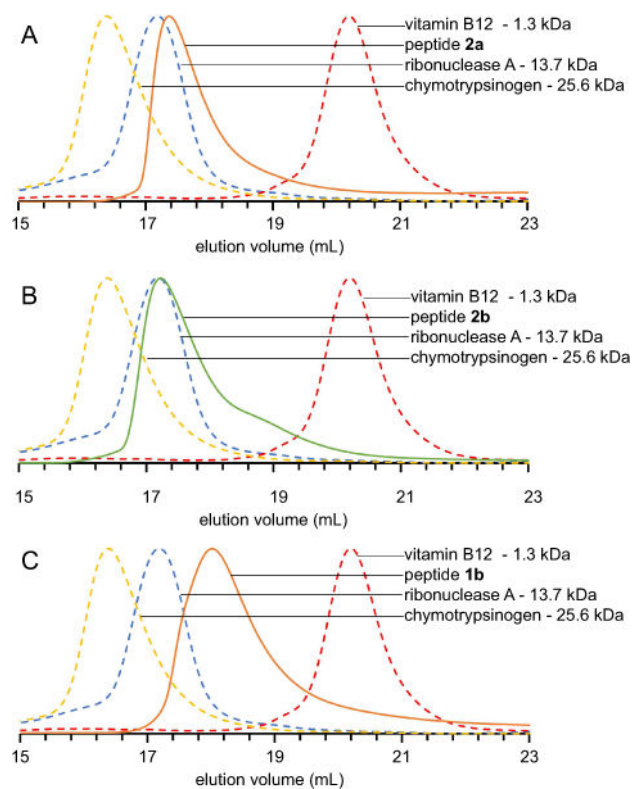


**Figure 7.** (A) SEC chromatograms of peptide **2a** (B) peptide **2b** (C) peptide **1b** chymotrypsinogen (yellow) ribonuclease A (blue) and vitamin B12 (red).

Table 1

Peptides 1 and 2 and Oligomers Observed Crystallographically.

peptide	R <sub>3</sub>	N-Me	R <sub>4</sub>	R <sub>5</sub>	oligomer	resolution (Å)
<b>1a</b>	Ala	Ala	Ala	Ala	hexamer	1.97
<b>1b</b>	Ala	Val	Ala	Ala	dodecamer	1.50
<b>1c</b>	Ala	Leu	Ala	Ala	dodecamer	1.90
<b>1d</b>	Ala	Ile	Ala	Ala	-	
<b>1e</b>	Ala	Nle	Ala	Ala	-	
<b>2a</b>	Thr	Ala	Thr	Thr	hexamer	1.51
<b>2b</b>	Thr	Val	Thr	Thr	octamer	1.31
<b>2c</b>	Thr	Leu	Thr	Thr	-	
<b>2d</b>	Thr	Ile	Thr	Thr	-	
<b>2e</b>	Thr	Nle	Thr	Thr	-	
<b>1a<sub>16SV</sub></b>	Ala	Ala	Ala	Ala	hexamer	2.02
<b>1a + 1c</b>	Ala	Ala/Leu	Ala	Ala	dodecamer	1.91

**Table 2**

SEC Elution Volumes MTT Conversion (%) and LDH Release (%) of Peptides 1 and 2.

peptide	SEC (mL)	MTT (%)	LDH(%)	crystallographic oligomer
<b>1a</b>	18.8 <sup>1</sup>	53±5	37±4	hexamer
<b>1b</b>	18.0	85±8	22±5	dodecamer
<b>1c</b>	17.6	54±15	45±6	dodecamer
<b>1d</b>	17.7	110±8	18±2	–
<b>1e</b>	17.6	42±5	44±7	–
<b>2a</b>	17.4	101±5	5±1	hexamer
<b>2b</b>	17.3	125±9	14±2	octamer
<b>2c</b>	17.8	34±3	38±5	–
<b>2d</b>	17.5	111±8	20±2	–
<b>2e</b>	17.3	49±4	36±4	–
Vitamin B12	20.3			
ribonuclease A	17.3			
chymotrypsinogen	16.5			